

Study of $c\bar{c}c\bar{c}$ and $c\bar{c}s\bar{s}$ at Belle

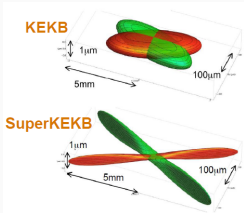
Dmytro Meleshko (*on behalf of Belle collab.*)

21.02.2024

Justus-Liebig-Universitaet, Giessen, Germany



From Belle to Belle II: experiment overview

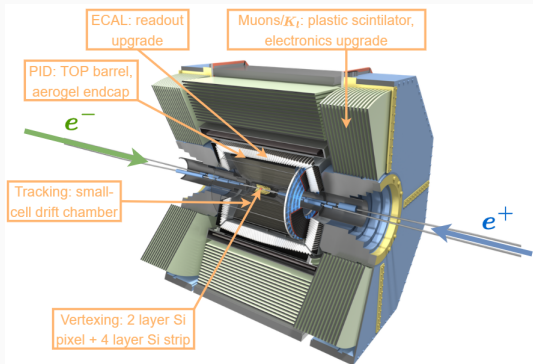


SuperKEKB:

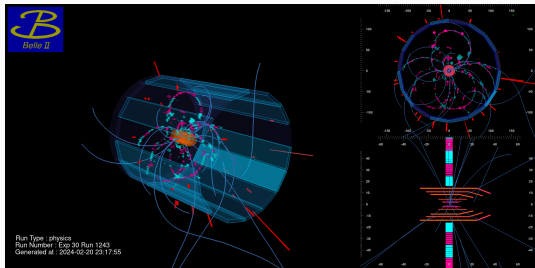
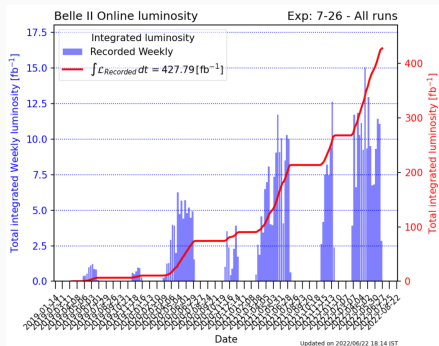
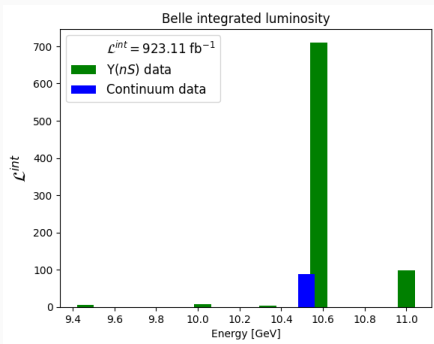
- Asymmetric e^+e^- collider at KEK (Tsukuba, Japan);
- Energy adjustment: 3.5/8.0 GeV (Belle) \rightarrow 7.0/4.0 GeV (Belle II);
- "Nano-beams" \times current increase ($\times 2$) = $\times 40$ inst. luminosity increase;

Belle II detector upgrade:

- Higher background:
 - Radiation damage;
 - Detector readout;
- Higher event rate (~ 30 kHz):
 - Trigger, DAQ, computing;
- Boost change:
 - Vertexing improvement;



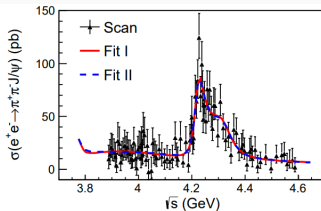
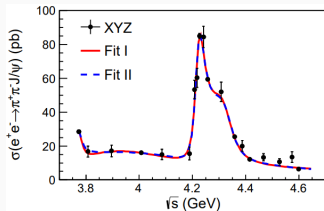
What data samples are available today?



20.02.2024 21:12 JST
First recorded collisions of Run 2

The puzzle of $Y(4260)$

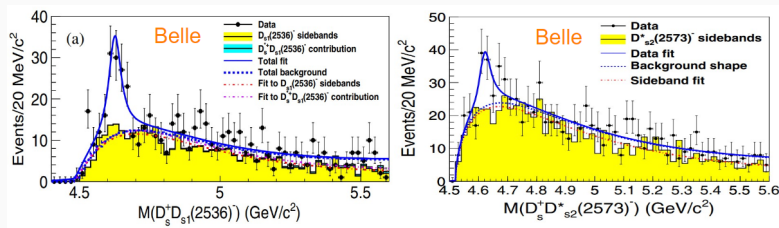
- A plethora of Y states ($J^{PC} = 1^{--}$) has been observed by B-factories while in parallel being extensively studied by theorists:
 - A $Y(4260)$ state with mass of $(4259 \pm 8_{-6}^{+2})$ MeV was observed in $e^+e^- \rightarrow \gamma_{ISR}\pi^+\pi^-J/\psi$ by BaBar (confirmed by Belle and CLEO);
Phys. Rev. Lett. 95, 142001 (2005) *Phys. Rev. D* 74, 091104 (2006) *Phys. Rev. Lett.* 99, 182004 (2007)
 - Lattice QCD calculation predicts $Y(4230)$ predicts it to have a mass of (4238 ± 31) MeV by treating it as a **molecule**. It also predicts existence of two additional states: $cs\bar{c}\bar{s}$ around (4450 ± 100) MeV and $cc\bar{c}\bar{c}$ around (6400 ± 50) MeV.
Phys. Rev. D 73, 094510 (2006)
 - BESIII study has shown that the s.c. $Y(4260)$ is not a simply a resonance, but two:
 - The $Y(4230)$ with the mass of $(4222.0 \pm 3.1 \pm 1.4)$ MeV and width of $(44.1 \pm 4.3 \pm 2.0)$ MeV *Phys. Rev. Lett.* 118, 092001 (2017) *Phys. Rev. Lett.* 118, 092002 (2017)
Phys. C 38, 043001 (2014) *Phys. Rev. D* 99, 091103 (2019) *Phys. Rev. Lett.* 122, 102002 (2019)
 - The $Y(4360)$ with the mass of $(4320.0 \pm 10.4 \pm 7.0)$ MeV and width of $(101.4_{-19.7}^{+25.3} \pm 10.2)$ MeV



Phys. Rev. Lett. 118, 092001 (2017)

Introduction

- **BESIII:** observation of a structure with the mass of $(4487.7 \pm 13.3 \pm 24.1)$ MeV in the cross-section measurements of $e^+e^- \rightarrow K^+K^-J/\psi$ (matches $c\bar{s}\bar{s}$ lattice QCD prediction);
Phys. Rev. D 97, 071101 (2018)
- **Belle:** observation of a structures with the masses of $(4625.9^{+6.2}_{-6.0} \pm 0.4)$ MeV and $(4619.8^{+8.9}_{-8.0} \pm 2.3)$ MeV in the cross-section measurements of $e^+e^- \rightarrow D_s^+D_{s1}(2536)^-$ and $e^+e^- \rightarrow D_s^+D_{s2}^*(2573)^-$ respectively
Phys. Rev. D 100, no.11, 111103 (2019) *Phys. Rev. D 101, no.9, 091101 (2020)*
- **LHCb:** a narrow peak near the double- J/ψ threshold (dubbed $X(6900)$, also confirmed by ATLAS and CMS) - $[QQ][\bar{Q}\bar{Q}]$?
Phys. Rev. Lett. 127, no.8, 082001 (2021) *Rept. Prog. Phys. 86 (2023) no.2, 026201*



**Search for the double-charmonium
state with $\eta_c J/\psi$ at Belle**

J.HighEnergy.Phys.2023, 121(2023)

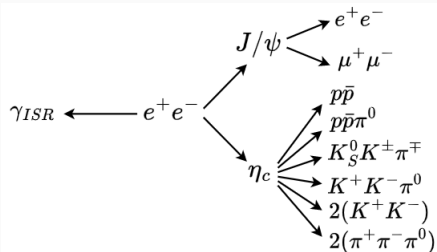
Search for the double-charmonium state with $\eta_c J/\psi$ at Belle

Motivation: $\eta_c J/\psi$ is the lowest mass combination of charmonia that a vector $cc\bar{c}\bar{c}$ can decay into. Might have large BF.

Data: 980 fb^{-1} ($\Upsilon(nS)$ and continuum)

Strategy:

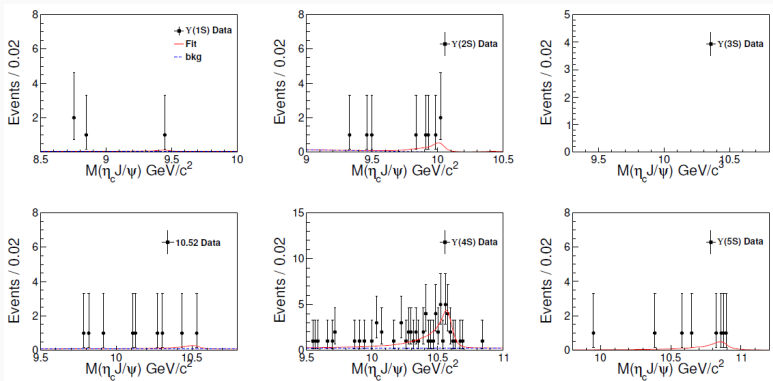
- ISR allows searching for $cc\bar{c}\bar{c}$ in the near-threshold region.
- Cross-section of $e^+e^- \rightarrow \eta_c J/\psi$ is first scanned on the $\Upsilon(nS)$ energy points:
 - analysis validation
 - NNLO nonrelativistic QCD approach check.
- Search for $\eta_c J/\psi$ and Y_{cc} is performed in the near-threshold region.
- Measured cross-sections are then extrapolated to the near-threshold region to the near-threshold region to check if potential signals are coming from continuum.



Exclusive reconstruction

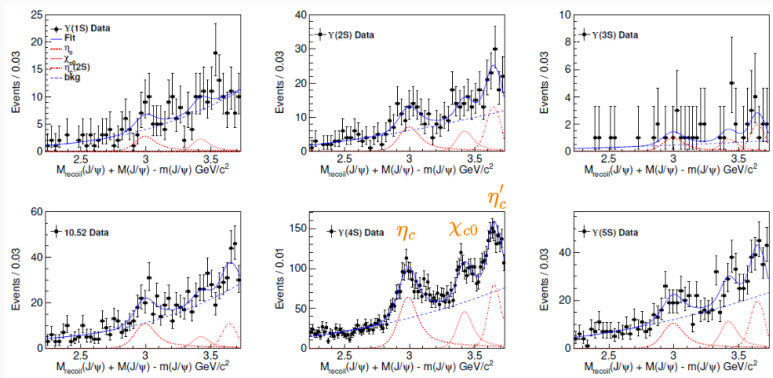
Cross-section calculation:

$$\sigma = \frac{N_{sig}}{\epsilon \mathcal{L} \mathcal{B}(J/\psi \rightarrow \ell^+ \ell^-) \mathcal{B}(\eta_c \rightarrow 6 \text{ channels})} \quad (1)$$



Inclusive reconstruction

- J/ψ recoil mass is studied: $M_{recoil}(J/\psi) \equiv \sqrt{|\mathbf{p}_{e^+e^-} - \mathbf{p}_{J/\psi}|^2}$
- $M_{recoil}(J/\psi) + M(J/\psi) - m(J/\psi)$ distribution is studied to achieve better resolution

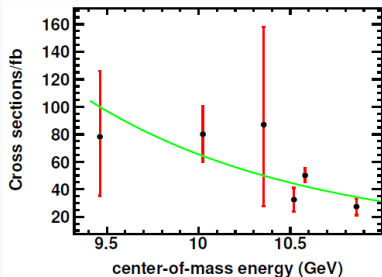


Search for the double-charmonium state with $\eta_c J/\psi$ at Belle

Continuum production fractions for $e^+e^- \rightarrow \mu^+\mu^-$ are about 5/6 and 4.5/4.75 for $\Upsilon(1S)$ and $\Upsilon(2S)$ datasets, respectively. For the other $\Upsilon(nS)$ they are taken as 1.

Fit function:

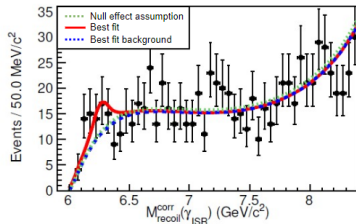
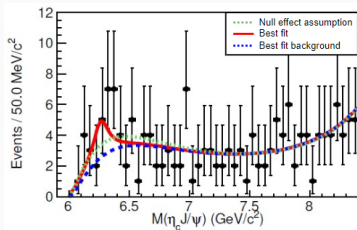
$$\sigma = A \frac{\sqrt{2\mu\Delta M}}{\left(\frac{s}{s_0}\right)^n}$$



	$\Upsilon(1S)$	$\Upsilon(2S)$	$\Upsilon(3S)$	10.52GeV	$\Upsilon(4S)$	$\Upsilon(5S)$
$\mathcal{L}[\text{fb}^{-1}]$	5.7	24.9	2.9	89.4	711.0	121.4
N^{exc}	$0.7^{+1.5}_{-0.9}$	$6.2^{+3.1}_{-2.3}$	< 1.9	$2.6^{+3.5}_{-2.5}$	$45.0^{+8.9}_{-8.2}$	$6.5^{+3.4}_{-2.7}$
ϵ^{exc}	8.3%	6.9%	5.7%	5.6%	5.6%	5.4%
$\sigma^{\text{exc}}[\text{fb}]$	$57^{+122}_{-73} \pm 6$	$140^{+70}_{-52} \pm 14$	< 442	$20^{+27}_{-19} \pm 6$	$44^{+9}_{-8} \pm 5$	$39^{+20}_{-14} \pm 7$
N^{inc}	23.7 ± 12.3	62.0 ± 17.9	8.5 ± 5.2	94.7 ± 23.8	1116.2 ± 62.9	91.1 ± 21.5
ϵ^{inc}	38.6%	29.6%	26.4%	26.1%	25.4%	24.7%
$\sigma^{\text{inc}}[\text{fb}]$	$89.1^{+46.2}_{-20.5}$	$70.1^{+20.2}_{-8.9}$	$91.8^{+56.2}_{-52.3}$	$33.8^{+8.5}_{-2.8}$	$52.1^{+2.9}_{-5.0}$	$25.4^{+6.0}_{-2.8}$
$\sigma^{\text{comb}}[\text{fb}]$	$78.3^{+47.5}_{-43.0}$	80.2 ± 20.4	$87.0^{+71.0}_{-59.0}$	32.5 ± 8.5	50.2 ± 5.0	27.5 ± 6.1

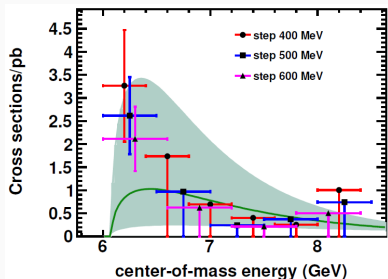
$e^+e^- \rightarrow \eta_c J/\psi$ near threshold

- Common events are removed from the inclusive reconstruction
- Signal count is 9 ± 4 and 23 ± 11 for exclusive and inclusive reconstructions
- The enhancement has a 2.1σ significance, located at (6267 ± 43) MeV mass and has a width of (121 ± 72) MeV



Search for the double-charmonium state with $\eta_c J/\psi$ at Belle

- The effective luminosity is calculated in each region
Phys. Lett. B 241, 278 (1990)
- $\pm 1\sigma$ area of the cross-section lineshape extrapolation is consistent with the threshold enhancement.



regions [GeV/ c^2]	$N_{\text{prod}} \times 10^2$	σ [pb]
[6.0, 6.4]	13.1 ± 3.6	$3.3 \pm 0.9 \pm 0.8$
[6.4, 6.8]	< 8.2	< 1.7
[6.8, 7.2]	< 3.9	< 0.7
[7.2, 7.6]	< 2.7	< 0.4
[7.6, 8.0]	< 2.1	< 0.3
[8.0, 8.4]	< 10.4	< 1.0
[6.0, 6.5]	13.4 ± 4.0	$2.7 \pm 0.8 \pm 0.2$
[6.5, 7.0]	< 6.1	< 1.0
[7.0, 7.5]	< 1.9	< 0.2
[7.5, 8.0]	< 3.8	< 0.4
[8.0, 8.5]	< 9.9	< 0.7
[6.0, 6.6]	13.3 ± 4.2	$2.1 \pm 0.7 \pm 0.2$
[6.6, 7.2]	< 5.0	< 0.6
[7.2, 7.8]	< 2.3	< 0.2
[7.8, 8.4]	< 7.4	< 0.5

**Observation of charmed strange
mesons pair production in $\Upsilon(2S)$
decays and in e^+e^- annihilation at
10.52 GeV**

Phys.Rev.D108, 112015(2023)

Observation of $c\bar{s} + \bar{c}s$ in $\Upsilon(2S)$ decays and at 10.52 GeV

Motivation:

- Study of the "off-resonance" data allows excluding QCD component and study QED-ruled production standalone.

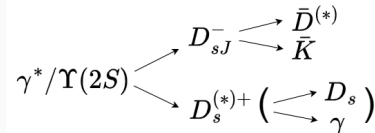
Background knowledge:

- $c\bar{c}$ constitutes about 40% of total hadronic production in continuum;
- Hadronic decays of $\Upsilon(nS)$ are OZI suppressed \rightarrow study is scarce;
 - BaBar reports $\mathcal{B}[\Upsilon(1S) \rightarrow D^{*\pm} X] = (2.52 \pm 0.13 \pm 1.15)\%$
at $(98.9 \pm 0.9) \times 10^6$ $\Upsilon(1S)$ events (Th: $\mathcal{B}[\Upsilon(1S) \rightarrow D^+ D^-] = 10^{-4} - 10^{-5}$).
[Phys. Rev. D 81 \(2010\) 011102](#) [Phys. Rev. D 74 \(2006\) 094016](#)
 - Theoretical predictions:
 - Splitting of a virtual gluon [Phys. Lett. B 77 \(1978\) 299](#)
 - Annihilation into an octet state [Phys. Rev. D 76 \(2007\) 051105](#)
 - NP process with exotic couplings to heavy quarks [Phys. Rev. D 81 \(2010\) 075017](#)

Observation of $c\bar{s} + \bar{c}s$ in $\Upsilon(2S)$ decays and at 10.52 GeV

Data:

- 24.7 fb^{-1} at $\Upsilon(2S) \sim (158 \pm 4) \times 10^6$ events
- 89.5 fb^{-1} at $\sqrt{s} = 10.52 \text{ GeV}$



$$* D_{sJ}^{(*)} = D_{s1}(2536) \text{ or } D_{s2}^{*}(2573)$$

Analysis strategy:

- Full reconstruction of $D_s^{(*)}$
- D_s decays into $\phi(\rightarrow K^+K^-)\pi^+$, $K_S^0(\rightarrow \pi^+\pi^-)K^+$, $\bar{K}^{*}(892)^0(\rightarrow K^-\pi^+)K^+$, $\rho(\rightarrow \pi^+\pi^0)\phi$ $\eta\pi^+$ and $\eta'\pi^+$ are reconstructed.
- Partial reconstruction for the D_{sJ}^- final state:
 - The flavor is determined with the produced K
 - The remaining $\bar{D}^{(*)}$ is observed indirectly through its recoil against the $D_s^{(*)} - K$ system using the known kinematics.
- Simulated D_{sJ}^- decay modes: $K^-\bar{D}^0$, $K_S^0D^-$, $K^-\bar{D}^{*}(2007)^0$ and $K_S^0D^{*}(2010)^-$

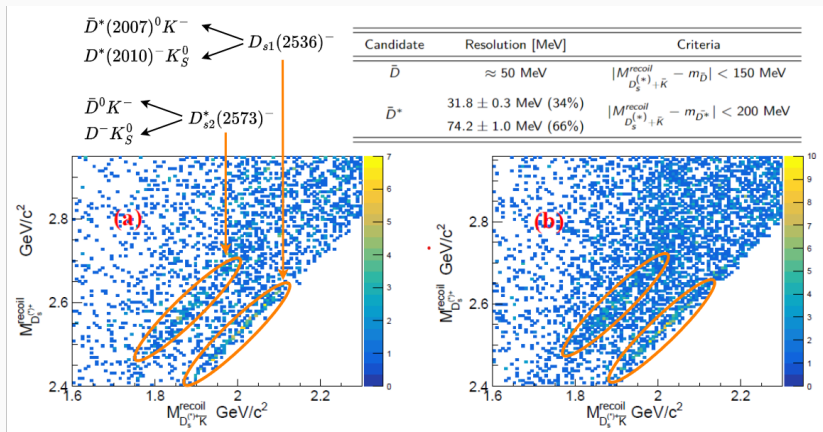
Observation of $c\bar{s} + \bar{c}s$ in $\Upsilon(2S)$ decays and at 10.52 GeV

$\bar{D}^{(*)}$ is determined through the recoil of $D_s^{(*)+} \bar{K}$:

$$M_{\bar{D}^{(*)}} = M_{D_s^{(*)+} \bar{K}}^{\text{recoil}} \equiv \sqrt{(E_{c.m.} - E_{D_s^{(*)+}} - E_{\bar{K}})^2 - (\vec{p}_{c.m.} - \vec{p}_{D_s^{(*)+}} - \vec{p}_{\bar{K}})^2} \quad (2)$$

And isolate production of D_{sJ}^- in the $\bar{K} \bar{D}^{(*)}$ final state through recoil defined as:

$$M_{\bar{K} \bar{D}^{(*)}} = M_{D_s^{(*)+}}^{\text{recoil}} \equiv \sqrt{(E_{c.m.} - E_{D_s^{(*)+}})^2 - (\vec{p}_{c.m.} - \vec{p}_{D_s^{(*)+}})^2} \quad (3)$$



Observation of $c\bar{s} + \bar{c}s$ in $\Upsilon(2S)$ decays and at 10.52 GeV

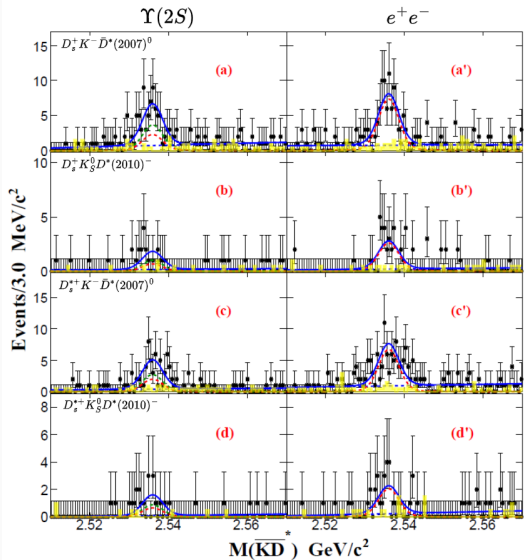
Large mass resolutions (due to the common variables in Eq. 2 and Eq. 3) can be cured by substituting Eq. 3 with:

$$M_{\bar{K}\bar{D}^{(*)}} = M_{D_s^{(*)+}}^{recoil} - M_{D_s^{(*)+}\bar{K}}^{recoil} + m_{\bar{D}^{(*)}} \quad (4)$$

$N_{\Upsilon(2S)}^{sig}$ and N_{cont}^{sig} for DsJ^- are estimated by fitting $M_{\bar{K}\bar{D}^{(*)}}$ distributions simultaneously with the common ratios $B(D_{sJ}^- \rightarrow K_S^0 D^{(*)-}) / (D_{sJ}^- \rightarrow K^- D^{(*)0})$ between the final states.

Fit function:

$$PDF = N_1 \cdot G(\mu_{D_{sJ}^-}^{PDG}, 2.4/6.5 \text{ MeV}) + N_2 \cdot BW(\mu_{D_{sJ}^-}^{PDG}, \sigma_{D_{sJ}^-}^{PDG}) \quad (5)$$



Observation of $c\bar{s} + \bar{c}s$ in $\Upsilon(2S)$ decays and at 10.52 GeV

The yield acquired on $\Upsilon(2S)$ can be interpreted as:

$$N_{tot}^{sig} = N_{\Upsilon(2S)}^{sig} + N_{cont}^{sig} \times \frac{\mathcal{L}_{\Upsilon(2S)} \cdot S_{cont}}{\mathcal{L}_{conr} \cdot S_{\Upsilon(2S)}} \quad (6)$$

Branching fractions and Born cross-sections calculation:

$$\mathcal{B}(\Upsilon(2S) \rightarrow D_s^{(*)+} D_{sJ}^-) \mathcal{B}(D_{sJ}^- \rightarrow \bar{K} \bar{D}^{(*)}) = \frac{N_{\Upsilon(2S)}^{sig} - f_{scale} \cdot N_{cont}^{sig}}{N_{\Upsilon(2S)} \times \sum \varepsilon_i \mathcal{B}_i} \quad (7)$$

$$\sigma^B(e^+ e^- \rightarrow D_s^{(*)+} D_{sJ}^-) \mathcal{B}(D_{sJ}^- \rightarrow \bar{K} \bar{D}^{(*)}) = \frac{N_{cont}^{sig} \times |1 - \Pi|^2}{\mathcal{L}_{cont} \times \sum \varepsilon_i \mathcal{B}_i \times (1 + \delta_{ISR})}$$

Final state (f)	$N_{\Upsilon(2S)}^{K^-}$	$\mathcal{B}_{\Upsilon(2S)f}^f \mathcal{B}_{D_{sJ}^-}^{K^- \bar{D}^{(*)0}} (\times 10^{-5})$	$S^{\Upsilon(2S)}$
$D_s^+ D_{s1}(2536)^-$	$43 \pm 9 \pm 2$	$1.4 \pm 0.3 \pm 0.1$	5.3
$D_s^{*+} D_{s1}(2536)^-$	$31 \pm 8 \pm 2$	$2.0 \pm 0.5 \pm 0.1$	4.3
$D_s^+ D_{s2}^*(2573)^-$	$51 \pm 15 \pm 5$	$1.6 \pm 0.5 \pm 0.1$	3.8
$D_s^{*+} D_{s2}^*(2573)^-$	$20 \pm 12 \pm 2$	$1.3 \pm 0.8 \pm 0.1$	1.6
Final state (f)	$N_{cont}^{K^-}$	$\sigma_{D_{sJ}^-}^{Born} \mathcal{B}_{D_{sJ}^-}^{K^- \bar{D}^{(*)0}} (\text{fb})$	S_{cont}
$D_s^+ D_{s1}(2536)^-$	$86 \pm 10 \pm 2$	$58 \pm 7 \pm 1$	13.9
$D_s^{*+} D_{s1}(2536)^-$	$79 \pm 10 \pm 2$	$101 \pm 13 \pm 2$	11.8
$D_s^+ D_{s2}^*(2573)^-$	$102 \pm 17 \pm 21$	$67 \pm 11 \pm 14$	7.1
$D_s^{*+} D_{s2}^*(2573)^-$	$102 \pm 16 \pm 6$	$126 \pm 20 \pm 7$	7.6

Curious takeaways:

1. The strong decay is expected to dominate in $\Upsilon(2S) \rightarrow D_s^{(*)+} D_{sJ}^-$ process:

$$R_1 \equiv \mathcal{B}(\Upsilon(2S) \rightarrow D_s^{(*)+} D_{sJ}^-) / \mathcal{B}(\Upsilon(2S) \rightarrow \mu^+ \mu^-)$$

$$R_2 \equiv \sigma^{\text{Born}}(e^+ e^- \rightarrow D_s^{(*)+} D_{sJ}^-) / \sigma^{\text{Born}}(e^+ e^- \rightarrow \mu^+ \mu^-)$$

$$R_1/R_2 = 9.8 \pm 2.5, 8.0 \pm 2.4, 9.7 \pm 3.0 \text{ and } 4.4 \pm 2.8$$

$$\text{(for } D_s^+ D_{s1}(2536)^-, D_s^{*+} D_{s1}(2536)^-, D_s^+ D_{s2}^*(2573)^- \text{ and } D_s^+ D_{s2}^*(2573)^-)$$

2. The ratios

$$\frac{\mathcal{B}(D_{s1}(2536)^- \rightarrow K_S^0 D^*(2010)^-)}{\mathcal{B}(D_{s1}(2536)^- \rightarrow K^- D^*(2007)^0)} = 0.59 \pm 0.08 \pm 0.02$$

$$\frac{\mathcal{B}(D_{s2}^*(2573)^- \rightarrow K_S^0 D^-)}{\mathcal{B}(D_{s2}^*(2573)^- \rightarrow K^- D^0)} = 0.64 \pm 0.12 \pm 0.04$$

are in good agreement with the expectation from isospin symmetry (with K_S^0 only half of the neutral kaons can be reconstructed).

Study of

$$e^+e^- \rightarrow D_s^+ D_{s0}^*(2317)^- A + \text{c.c.}$$

$$\text{and } e^+e^- \rightarrow D_s^+ D_{s1}(2460)^- A + \text{c.c}$$

at Belle

PRELIMINARY

Study of $e^+e^- \rightarrow D_s^+ D_s^- A + \text{c.c.}$ at Belle

Invariant mass system	Decay from:	Range [GeV/ c^2]
$D_s^- D_s^+$	B_s^0	[3.936 - 5.298]
$D_s^- D_s^+ \pi^0$	B_s^0	[4.071 - 5.433]
$D_s^- D_s^{*+}$	B_s^0	[4.080 - 5.433]
$D_s^- D_{s0}^*(2317)^+$	B_s^0	[4.285 - 5.433]
$J/\psi\phi$	B^0	[4.117 - 4.783]
$J/\psi\phi$	B^\pm	[4.117 - 4.783]
$J/\psi\phi$	continuum	all range
$D_s^- D_{s0}^*(2317)^+, D_s^- D_{s1}(2460)^+, D_s^- D_s^+ \pi^0, D_s^- D_s^{*+}$	continuum	all range

$$\left. \begin{array}{l} D_s^- D_s^+ \\ D_s^- D_s^+ \pi^0 \\ D_s^- D_s^{*+} \\ D_s^- D_{s0}^*(2317)^+ \end{array} \right\} B_s^0 \rightarrow D_s^{(*)+} D_s^{(*)-} \pi^0$$

$$\left. \begin{array}{l} J/\psi\phi \\ J/\psi\phi \end{array} \right\} B^{0,\pm} \rightarrow J/\psi\phi K^{0,\pm}$$

$$e^+e^- \rightarrow J/\psi\phi + \text{anything}$$

$$e^+e^- \rightarrow D_s^{(*)+} D_s^{(*)-} + \text{anything}$$

X(4274)

X(4685)

X(4630)

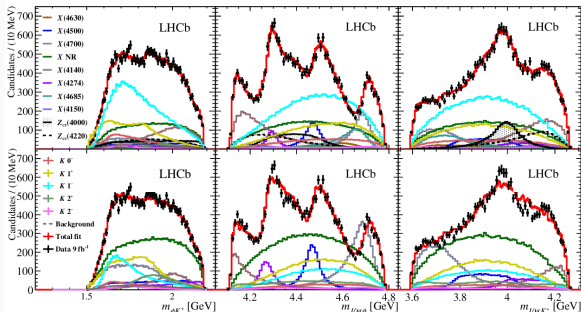
X(4500)

X(4700)

LHCb results:

- 9 fb^{-1} of data
- 7 neutral X states
- 3 charged Z states

Phys. Rev. Lett. 127, 082001



Study of $e^+e^- \rightarrow D_s^+ D_{sJ}^- A + \text{c.c.}$ at Belle

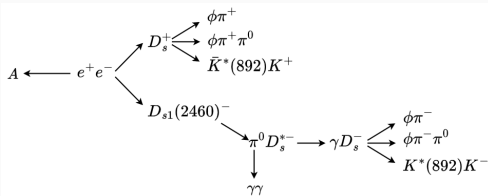
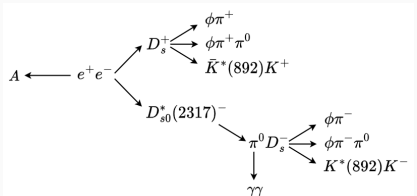
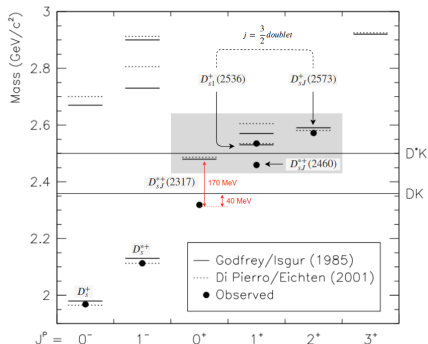
First $e^+e^- \rightarrow D_s \pi^0 X$ process studies:

- BaBar: 1267 yield on 91 fb^{-1}
- Belle: 761 yield on 87 fb^{-1}

Extrapolation from the old analysis with $D_s^*(2317)$ only, but to the whole data set:

- Belle @ $\Upsilon(4S)$: 6226 **Only $D_s^*(2317)$!**

With one extra D_s (e.g. +3 charged tracks), efficiency is expected to drop ($< 1\%$). Around 100 events are expected on full Belle dataset.



Signal MC

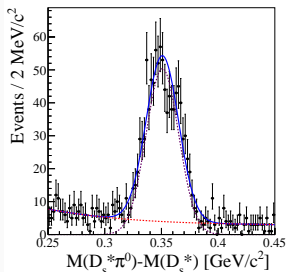
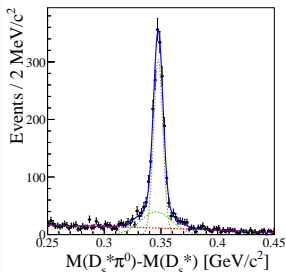
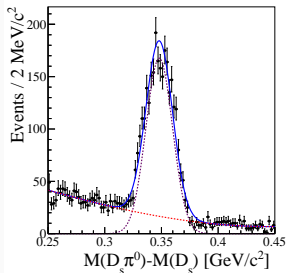
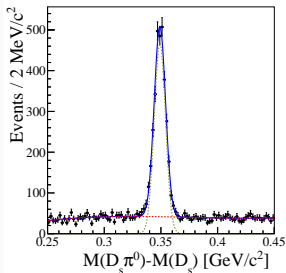
The following peaking contributions are expected

$D_{sJ}(2317)^+$ invariant mass region:

- True $D_{sJ}(2317)^+$ peak
 $\sigma = (4.76 \pm 0.8) \text{ MeV}$
- $D_{sJ}(2460)^+$ reflection peak
 $\sigma = (11.8 \pm 0.3) \text{ MeV}$

$D_{sJ}(2460)^+$ invariant mass region:

- True $D_{sJ}(2460)^+$ peak
 $\sigma = (5.07 \pm 0.13) \text{ MeV}$
- $D_{sJ}(2317)^+$ reflection peak
 $\sigma = (14.6 \pm 0.7) \text{ MeV}$
- $D_{sJ}(2460)^+$ "broken signal"
 $\sigma = (16.9 \pm 1.8) \text{ MeV}$



Study of $e^+e^- \rightarrow D_s^+ D_s^- A + \text{c.c.}$ at Belle

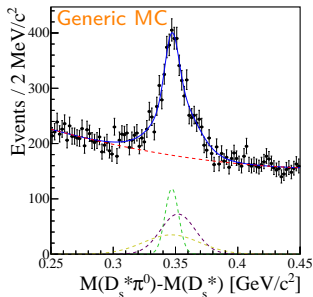
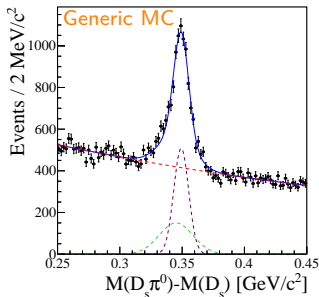
$$\Delta M(D_s \pi^0) = N_1 G(\mu_1, \sigma_1) + f^{\text{down}} N_2 G(\mu^{\text{down}}, \sigma^{\text{down}}) \quad (8)$$

$$\Delta M(D_s^* \pi^0) = N_2 G(\mu_2, \sigma_2) + f^{\text{up}} N_1 G(\mu^{\text{up}}, \sigma^{\text{up}}) + f^{\text{broken}} N_2 G(\mu^{\text{broken}}, \sigma^{\text{broken}})$$

ref: $N = 3,843 \pm 67$, $\mu = 348.9 \pm 0.1$, $\sigma = 6.20 \pm 0.10$

ref: $N = 835 \pm 31$, $\mu = 347.1 \pm 0.2$, $\sigma = 5.80 \pm 0.20$

Topology type	μ , [MeV]	σ , [MeV]	N
True D_{s0}^* (2317) signal	349.3 ± 0.2	5.97 ± 0.25	$3,797 \pm 137$
Feed-down background	345.1 (fixed)	13.5 (fixed)	$0.3297 \cdot N_2$
True D_{s1} (2460) signal	347.1 ± 0.5	5.46 ± 0.60	811 ± 155
Feed-up background	352.0 (fixed)	13.9 (fixed)	$3.042 \cdot N_1$
D_{s1} (2460)	346.7 (fixed)	22.7 (fixed)	$1.189 \cdot N_2$



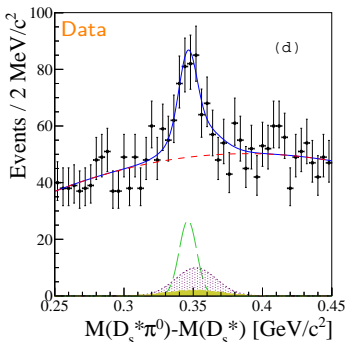
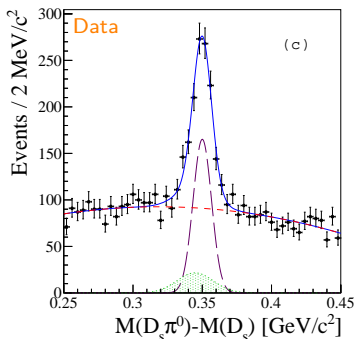
Study of $e^+e^- \rightarrow D_s^+ D_{sJ}^- A + \text{c.c.}$ at Belle

Cut-based selection \rightarrow MVA selection

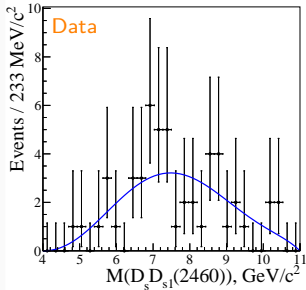
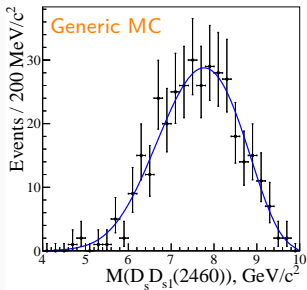
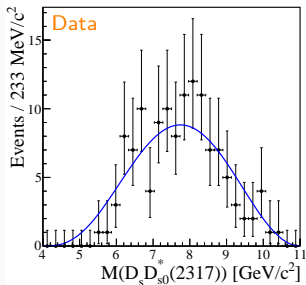
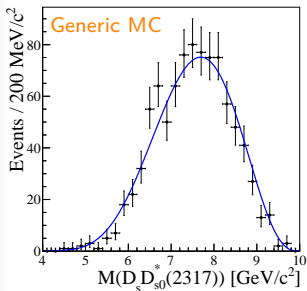
Topology type	μ , [MeV]	σ , [MeV]	N
True D_{s0}^* (2317)	350.0 ± 0.5	6.64 ± 0.53	688 ± 62
Feed-down bkg.	344.8 (fixed)	13.1 (fixed)	$1.688 \cdot N_2$
True D_{s1} (2460)	346.2 ± 1.7	6.27 ± 1.55	105 ± 27
Feed-up bkg.	351.9 (fixed)	14.8 (fixed)	$0.134 \cdot N_1$
Broken signal	351.0 (fixed)	20.4 (fixed)	$0.247 \cdot N_2$

Cuts: $N(D_{s0}^*(2317)) = 370 \pm 45$

$N(D_{s1}(2460)) = 68 \pm 22$



Study of $e^+e^- \rightarrow D_s^+ D_{sJ}^- A + \text{c.c.}$ at Belle



Study of $e^+e^- \rightarrow D_s^+ D_{sJ}^- A + \text{c.c.}$ at Belle

$$\frac{Br(D_{s1}(2460) \rightarrow D_s^* \pi^0)}{Br(D_{s0}^*(2317) \rightarrow D_s \pi^0)} \times \frac{\sigma(D_{s1}(2460), \text{MVA})}{\sigma(D_{s0}^*(2317), \text{MVA})} = 0.26 \pm 0.07(\text{stat}) \pm 0.03(\text{syst})$$

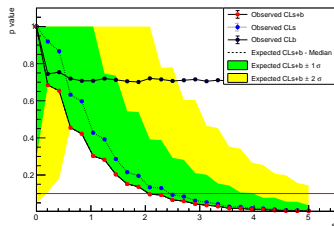
*The value earlier measured by Belle is $0.29 \pm 0.06 \pm 0.03$

**The value predicted by theory is 3

$$\sigma(e^+e^- \rightarrow D_s^+ D_{sJ}^{(*)-} A) \mathcal{B}(D_s^- \rightarrow 3 \text{ modes}) \mathcal{B}(D_s^+ \rightarrow 3 \text{ modes}) = \frac{N^{UL} \times |1 - \Pi|^2}{\mathcal{L} \times \sum_{ij} \epsilon_{ij}^* \mathcal{B}_i \mathcal{B}_j \times (1 + \delta)_{ISR}}$$

Curious takeaways:

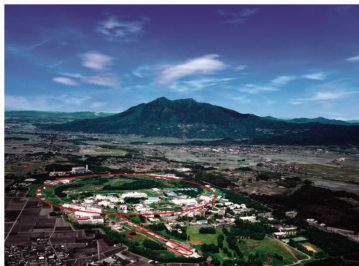
- The estimated ratio of branching fractions is consistent with earlier Belle study.
- $D_s D_{sJ}$ invariant mass distributions on data appeared to be PHSP-distributed.
- Cross-section UL for the accessible X states are evaluated.



Decay chain	Total error [%]	Estimated N_{90}^{UL}	$\sigma^{UL} \times \mathcal{B}(X \rightarrow D_s D_{sJ}^*)$ [fb^{-1}]
$e^+e^- \rightarrow X(4274)A$	13.3	2.45	122.5
$e^+e^- \rightarrow X(4685)A$	14.1	2.04	101.8
$e^+e^- \rightarrow X(4630)A$	18.3	2.05	228.1
$e^+e^- \rightarrow X(4500)A$	18.0	2.34	260.1
$e^+e^- \rightarrow X(4700)A$	18.7	2.18	241.8

Summary

1. No significant signal is seen in the $e^+e^- \rightarrow \eta_c J/\psi$ process near threshold. The observed enhancement can be explained by continuum contribution.
2. Born cross-sections and branching fractions are measured for the $e^+e^-/\Upsilon(2S) \rightarrow D_s^{(*)+} D_{sJ}^-$ processes. This allows to conclude about the intrinsic features of $\Upsilon(2S)$ decays.
3. No significant signal is seen in the $D_s D_{sJ}^{(*)}$ system. Upper limits on the accessible X states that were earlier reported by LHCb are set.



Backup

Observation of $c\bar{s} + \bar{c}s$ in $\Upsilon(2S)$ decays and at 10.52 GeV

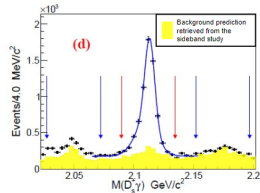
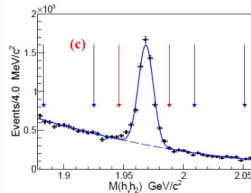
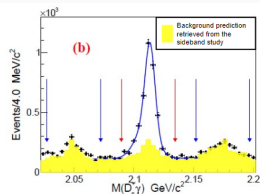
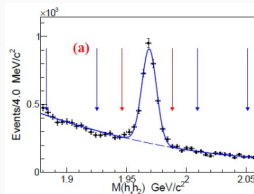
- Cut-based selection is developed for the $D_s^{(*)-}$ candidates;
- D_s^- invariant mass fit:

$$\sigma_{D_s^-} = 7.0 \pm 0.1 \text{ MeV}$$

- BCS applied on D_s^{*-} candidates leads to peaking background (studied in a side-band).

Fit performed:

$$\sigma_{D_s^{*-}} = 6.7 \pm 0.4 \text{ MeV}$$



Search for the double-charmonium state with $\eta_c J/\psi$ at Belle

- $M_{recoil}^2 = |p_{e^+e^-} - p(\eta_c) - p(J/\psi)|^2$;
- At least four charged tracks are required in the inclusive reconstruction to suppress QED background;

Candidate	Criteria
	$dr < 1.0$ cm
All tracks	$ dz < 4$ cm
	$p_T > 100$ MeV
K	$\mathcal{L}_K / (\mathcal{L}_K + \mathcal{L}_\pi) > 0.6$
p	$\mathcal{L}_p / (\mathcal{L}_p + \mathcal{L}_\pi) > 0.6$
μ	$\mathcal{L}_p / (\mathcal{L}_p + \mathcal{L}_K) > 0.6$
e	$\mathcal{L}_\mu / (\mathcal{L}_\mu + \mathcal{L}_p + \mathcal{L}_K) > 0.6$
	$\mathcal{L}_e / (\mathcal{L}_e + \mathcal{L}_{non-e}) > 0.01$
γ_{ISR}	$E_\gamma > 1$ GeV
K_S^0	NN
	$E_\gamma > 25$ MeV (barel)
π^0	$E_\gamma > 50$ MeV (endcap)
	$155 < M_{\gamma\gamma} < 155$ MeV
γ^{BS}	50 mrad cone
J/ψ	$3 < M(e^+e^-) < 3.12$ GeV
	$3.075 < M(\mu^+\mu^-) < 3.125$ GeV
η_c	$2.78 < M(\eta_c) < 3.08$ GeV
BCS	$\min(M_{\eta_c J/\psi}^{recoil})$

Observation of $c\bar{s} + \bar{c}s$ in $\Upsilon(2S)$ decays and at 10.52 GeV

Candidate	Resolution [MeV]	Criteria
Tracks	-	$dr < 1.5$ cm $ dz < 5$ cm $p_T > 0.1$ GeV $\mathcal{L}_K > 0.6$ $\mathcal{L}_\pi > 0.4$
K_S^0	≈ 5	$ M_{\pi^+\pi^-} - m_{K_S^0} < 3\sigma$ NN
ϕ	≈ 3.3	$ M_{K^+K^-} - m_\phi < 3\sigma$
$K^*(892)$	$\ll 47.3$	$ M_{K^-\pi^+} - m_{K^*(892)} < 105$ MeV
ρ^+	$\ll 150$	$ M_{\pi^+\pi^0} - m_\rho < 200$ MeV
π^0	≈ 5	$ M_{\gamma\gamma} - m_{\pi^0} < 3\sigma$ MeV $E_\gamma > 25$ MeV (barel)
γ	-	$E_\gamma > 50$ MeV (endcap)
η	≈ 4 ($\rightarrow \pi^+\pi^-\pi^0$) ≈ 13.4 ($\rightarrow \gamma\gamma$)	$ M_{\pi^+\pi^-\pi^0} - m_\eta < 3\sigma$ $ M_{\gamma\gamma} - m_\eta < 3\sigma$ $E_\gamma > 100$ MeV
η'	≈ 5	$ M_{\eta\pi^+\pi^-} - m_{\eta'} < 3\sigma$
D_s	7.9 ± 0.1	$ M_{h_1h_2} - m_{D_s} < 3\sigma$
D_s^*	6.7 ± 0.4	$ M_{\gamma D_s} - m_{D_s^*} < 50$ MeV $E_\gamma > 50$ MeV (barel) $E_\gamma > 100$ MeV (endcap) BCS: $\min(\chi^2)$

Signal MC. Optimized selection and BCS implementation.

In addition to the selection summarized on the right, the BCS selection was applied in the latest iteration of a study.

Selection optimization study has been conducted.

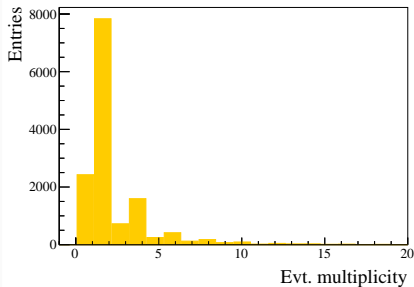


Figure 1: Signal MC. Event multiplicity before BCS application.

Particle	Selection criterion
Tracks	$dr < 0.5 \text{ cm}$
	$dz < 3 \text{ cm}$
	$P_{K_1}(K/\pi) > 0.5$
	$P_{K_2}(K/\pi) > 0.2$
π^0	$P_{\pi}(K/\pi) < 0.9$
	$E(\gamma) > 100 \text{ MeV}$
	$p(\gamma\gamma) > 150 \text{ MeV}/c$
	$\chi^2(\gamma\gamma) < 200$
ϕ	$122 < M(\gamma\gamma) < 148 \text{ MeV}/c^2$
	$P_{\chi^2}(\gamma\gamma) > 1\%$
	$1.010 < M(KK) < 1.030 \text{ GeV}/c^2$
$K^*(892)$	$P_{\chi^2}(KK) > 0.1\%$
	$842 < M(K\pi) < 942 \text{ MeV}/c^2$
D_s	$P_{\chi^2}(K\pi) > 0.1\%$
	$1.9585 < M(D_s) < 1.9785 \text{ GeV}/c^2$
$D_{s0}^*(2317)$	$P_{\chi^2}(D_s) > 0.1\%$
	$p^*(D_s\pi^0) > 2.79 \text{ GeV}/c$
Other	$P_{\chi^2}(D_s\pi^0) > 0.1\%$
	$ \cos\theta_H > 0.42$

Table 1: The summarized selection for $D_{s1}(2460)$ reconstruction.

* γ_* denotes the photon combined with D_s to create D_s^* candidate decaying into $D_s\gamma$.

Signal MC. $D_s D_{s0}^*(2317)$ system study (threshold case).

$$\epsilon = 0.22 \pm 0.02\%$$

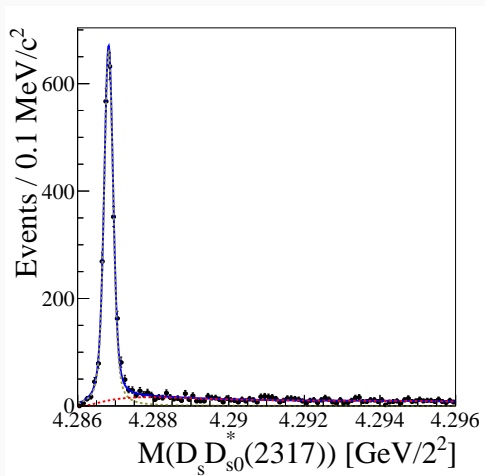


Figure 2: The $D_s D_{s0}^*(2317)$ invariant mass distribution in threshold case. The signal contribution is fitted by Voigt function, non-resonant background as approximated by the Threshold function.

MVA methods comparison

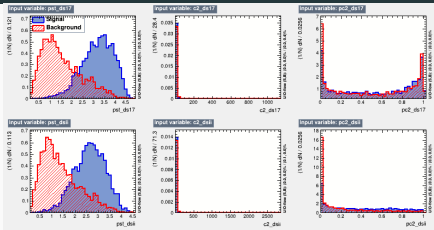


Figure 3: MVA input variables for signal (blue) and background (red) events.

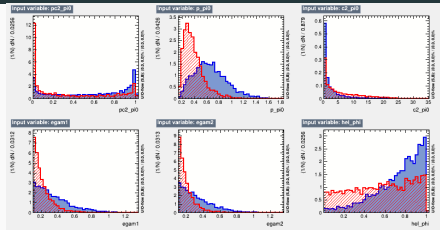


Figure 4: MVA input variables for signal (blue) and background (red) events.

- Pre-selection is applied.
- Performances of MLP, BDT, Fisher and DNN methods are compared → **MLP is chosen**
- Set of input variables is optimized with respect to correlation matrix → **redundant variables eliminated.**

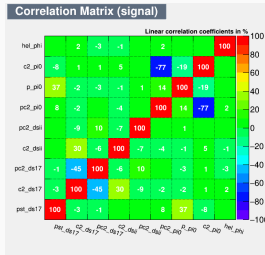


Figure 5: Input parameters Correlation Matrix for signal events.

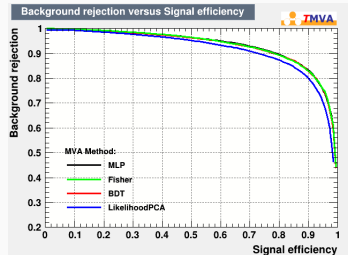


Figure 6: ROC curve.

MLP application

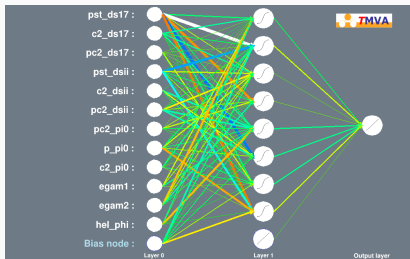


Figure 7: MLP architecture.

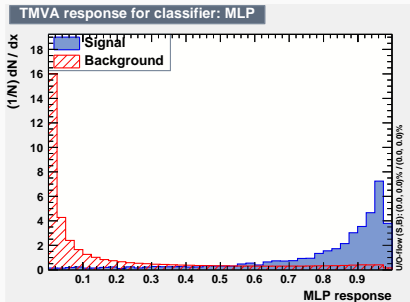


Figure 8: MLP response for classifier on training sample.

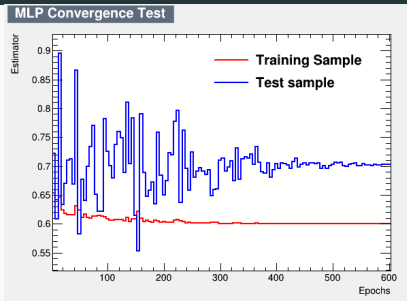


Figure 9: MLP convergence test.

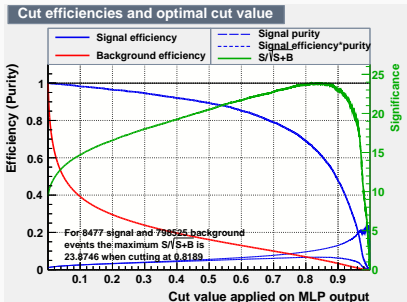


Figure 10: FoM dependence on classifier cut value.

Systematic uncertainties

Systematic Contribution	$D_s D_{s0}^*(2317)$ %	$D_s D_{s1}(2460)$ %
Charged tracks identification	3.21	3.21
Track reconstruction	2.10	2.10
MC statistics	1.82	2.42
Integrated luminosity	1.40	1.40
π^0 reconstruction	2.00	2.00
γ reconstruction	-	2.30
Secondary BF	5.83	5.62
Background fit PDF order	1.03	1.23
Mass cuts on secondary particles	5.58	7.80
TOTAL	9.50	11.22

Asymptotic method

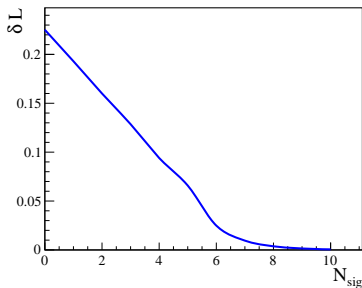
Equation to solve:

$$\frac{\int_0^{N^{90\%}} \mathcal{L}(x) dx}{\int_0^{+\infty} \mathcal{L}(x) dx} = 0.9 \quad (9)$$

$N^{90\%}$ - wanted UL on the number of signal events.

Target dependency to study:

$$\Delta L = e^{\mathcal{L}(N_{sig}) - \mathcal{L}_0} \quad (10)$$



Consideration of the systematic uncertainties:

$$\Delta(\Delta L) = \frac{\Delta \mathcal{L}_j \cdot \mathcal{L}_j}{\sqrt{2\pi \varepsilon_{syst} N_j^{sig}}} \cdot e^{-\frac{1}{2} \left(\frac{\Delta N_j^{sig}}{\varepsilon_{syst} N_j^{sig}} \right)^2} \quad (11)$$

Cross-section UL calculation:

$$\sigma^{90\%} = \frac{N^{90\%}}{\varepsilon^{tot} \cdot \mathcal{L}^{int}} \quad (12)$$

Likelihood ratio:

$$\lambda(\mu) = \frac{\mathcal{L}(\mu, \hat{\theta} | n_1, \dots, n_{N_b})}{\mathcal{L}(\mu, \hat{\theta} | n_1, \dots, n_{N_b})}, \quad (13)$$

where $(\mu, \hat{\theta})$ are the parameters that maximize the likelihood for the set of observations n_1, \dots, n_{N_b} ; and $\hat{\theta}$ maximizes the likelihood for a given value of μ .

Test statistics q_μ :

$$q_\mu = \begin{cases} -2 \ln \lambda(\mu) & \text{if } \mu > \hat{\mu}, \\ 0 & \text{otherwise} \end{cases} \quad (14)$$

The level of agreement between the data and the hypothesized value of μ is quantified with the p -value:

$$p_{s+b} = P(q_\mu > q_{\mu, \text{obs}} | \mu) = \int_{q_{\mu, \text{obs}}}^{\infty} p(q_\mu | \mu) dq_\mu, \quad (15)$$

where $> q_{\mu, \text{obs}}$ is the observed value of q_μ , and $p(q_\mu | \mu)$ denotes the probability density function of q_μ under the assumption of a signal strength of μ .

UL on μ at 90% CL is the largest value of μ such as p_{s+b} stays above 0.1

